Cost Optimization of a Symbiotic System to Harvest Uranium from Seawater via an Offshore Wind Turbine

Margaret Flicker Byers[a], Maha N. Haji[b,*], Alexander H. Slocum[b], Erich Schneider[a]

[a] *Department of Mechanical Engineering, Nuclear and Radiation Engineering Program, University of Texas, Austin*
[b] *Department of Mechanical Engineering, Massachusetts Institute of Technology*

Abstract

The recovery of uranium from seawater has the potential to transform the perceived sustainability of energy generated by uranium intensive nuclear fuel cycles, while providing environmental benefits as compared to land-based mining. Combining a seawater uranium harvester with an existing offshore wind turbine allows for denser energy recovery per unit ecosystem, as well as lowering the uranium production cost. The analysis presented in this paper focuses on the economic impacts on uranium recovered by adsorbing material deployed with such a symbiotic system as compared to a reference kelp-field like deployment. The Wind and Uranium from Seawater Acquisition symBiotic Infrastructure (WUSABI) was subjected to an independent economic analysis and design optimizations in an effort to reduce the seawater uranium cost. In addition to providing greater transparency to previous economic analyses of this system, this work alters chemical tank materials and establishes a novel means of calculating and optimizing the interval in which symbiotic systems are serviced. The perturbations proposed in this work could achieve a cost savings of 30% as compared to uranium produced from the reference kelp-field like deployment system. Additional design sensitivities are also explored to identify major cost drivers and guide future work regarding deployment location of the turbine field.

Keywords: nuclear power, offshore wind turbine, uranium, optimization, symbiotic system, systems analysis

*Corresponding author
Email addresses: meflicker@utexas.edu (Margaret Flicker Byers), mhaji@mit.edu (Maha N. Haji), slocum@mit.edu (Alexander H. Slocum), eschneider@mail.utexas.edu (Erich Schneider)

1. Introduction

Extraction of uranium from seawater has been researched for decades, with one of the first studies conducted by [10] after World War II in an effort to secure a uranium supply for Britain at a time when the existence of and access to abundant uranium resources was uncertain. Although evidence indicates that conventional terrestrial mining can satisfy world requirements at moderate cost for the next several decades, the ability to economically recover the 4 billion tonnes of uranium naturally existing in the ocean would assure very long-term availability and accessibility of this critical material. In addition to establishing supply security, this would reduce the uncertainty associated with fuel costs, providing policy and decision makers with increased confidence in the long-term viability of nuclear power. Sea- water uranium can also be considered a hedge against the possibility of future uranium scarcity or price hikes, and may be achieved at a considerably lower cost and without concerns for proliferation associated with breeder reactors which utilize plutonium.

A review article [28] details the evolution of technologies proposed since the 1960s for recovering uranium from seawater as well as their production cost estimates. Two primary components of seawater uranium production cost are adsorbent synthesis and ocean deployment of the adsorbent. In general, the synthesis cost and the adsorbent's capacity for taking up uranium are seen to be the most significant drivers of seawater uranium production cost, but deployment cost is also significant; and deployment costs grow in relative importance as the adsorbent material improves. Modern adsorbents are characterized by increasing durability and can thus be reused in the sea multiple times, with deployment costs incurred upon each reuse.

Both [28] and a recent review of proposed uranium recovery technologies by [22] identified uranium adsorption by chelating polymers [45, 36, 1] to be the most promising in terms of cost, adsorption capacity, and environmental footprint. Other techniques including membrane filtration, coagulation, and precipitation [21, 41, 40] were found to have issues such as high operating costs, poor durability, or toxicity. Further, [28] noted that the deployment strategies involving active pumping of seawater required an implausibly large portion of the uranium contained in the circulated water be captured for the strategy to approach economic viability. For that reason, recent work has focused on systems where passive mechanisms, typically natural circulation present in the oceans, provide sufficient seawater exposure to the adsorbent.

These passive strategies envision deployment of adsorbent at moderate depth and distance from coastlines, so costs associated with the system to moor the adsorbent to the seabed can be substantial. This work assesses the potential cost savings from leveraging existing structures, specifically offshore wind turbines, to serve as mooring platforms for the adsorbent.

Given that the focus of this analysis is the cost savings associated with the novel marine deployment structure, the adsorbent synthesis and necessary post-processing is modeled identically in all cases, and not covered in great detail. All uranium production costs presented here are calculated using the consistently strong performing and well documented amidoxime-based ligands under continued development by Oak Ridge (ORNL) [9, 6, 7]. These adsorbent fibers consist of high density polyethylene synthesized by radiation-induced graft polymerization to attach a hydrophilic functional group and the amidoxime ligand, which affords the uranium affinity. The fibers are then braided before being sent out to sea for their soaking campaign, after which they are removed to the surface so the uranium may be eluted off. These robust adsorbents can then be regenerated with a sodium hydroxide rinse and returned to the ocean for multiple subsequent soaking and elution cycles [25, 30]. This uranium recovery methodology will be applied to both the leading conventional deployment strategy as well as the novel symbiotic system, both of which will be described in more detail in section 2.

2. Alternate Recovery Strategies

This analysis builds upon the technology identified by [22] developed by a consortium led by ORNL and Pacific Northwest National Labs (PNNL). Under this approach, polymer fibers are grafted with uranium chelating ligands to allow for the passive extraction of uranium from seawater by adsorption. The optimal immersion time in seawater of the polymer-based adsorbents is on the order of several days to weeks. This reflects a trade off between factors including diminishing adsorption rates as the saturation capacity is approached, and the required extent of the adsorbent field in order to produce uranium at the desired rate, as well as the cost incurred each time the adsorbent is deployed. Once the adsorbent is recovered from the sea, elution is used to strip the uranium from the polymers. The adsorbent polymer may undergo a number of elution cycles before being disposed of or recycled for the scrap value of the polymer. The output from the elution process undergoes purification and precipitation typical for mined uranium to produce yellowcake.

Several of the polymer adsorbent system concepts have been subject to marine tests to evaluate performance, feasibility and cost-effectiveness. The Japanese Atomic Energy Agency (JAEA) first developed a system of buoy floated stacks of adsorbent fabric. However, due to the weight of the mooring equipment, mooring operations were found to account for more than 70% of the cost of this concept [38, 36]. In addition, the adsorbent was to be brought back to shore for the elution process and redeployed afterward. These stand-alone intermittent operation systems have significant practical and economic deployment challenges [36] and to date none have proven economically viable.

To address this problem, a buoyant braid adsorbent made of polyethylene fibers on a polypropylene trunk was proposed by [39]. This system requires adsorbents to be braided into 60 meter long segments. Braids are shipped out to sea where they are moored to the ocean floor using anchoring chains to form a kelp-field like structure. After sufficient exposure to seawater, their soaking campaign ends and the braids are winched up to the surface by workboats for elution. This design was found to achieve a reduction of 40% in the cost of uranium recovery compared to the adsorbent stack system, resulting in an estimated uranium production cost of $1000/kg U [39]. An independent cost-analysis by [35] of the system yielded a production cost of $1230/kg U (both figures are in year 2011 dollars). Much of the difference in cost was attributed to the second paper's inclusion of an experimentally observed 5% degradation of adsorbent capacity per use cycle. Further sensitivity studies confirmed that the major cost divers of such a system were the adsorbent capacity, number of recycles, and capacity degradation. For instance, if the capacity of the adsorbent was increased from 2 kg U/tonne adsorbent to 6 kg U/tonne adsorbent and the number of recycles was increased from 6 to 20, with no degradation and unchanged adsorbent production costs, the uranium production cost was estimated to drop to ca. $300/kg U [35]. In comparison, the market price of uranium has ranged from a 2016 low of near $60/kg U to a peak of $300/kg U in 2007 when demand for nuclear power was higher.[33] cites that nuclear reactors which require reprocessed uranium for fuel (also known as breeder reactors) have a breakeven price of $210-$560/kg U. Hence, one goal is to determine if the production price of seawater uranium would become cost competitive with breeder reactor technologies, which currently account for almost 5% of new nuclear fuel [42].

To date, the use of buoyant adsorbents in the kelp-field like structure has been regarded as the best available and served as the status quo in many previous analyses [9, 6, 7, 38, 39, 35, 34] of recovery system costs. However,

this paper focuses on performance modeling as well as cost and system analysis of a proposal by [32], who proposed a deployment method that couples a uranium adsorbent system with offshore wind turbines. The Wind and Uranium from Seawater Acquisition symBiotic Infrastructure (WUSABI) utilizes existing marine infrastructures to moor the adsorbent as well as to provide a platform and supply of energy to enable the chemical processing involved in recycling the adsorbent and recovering uranium from it.

These innovations are aimed at reducing the cost floor imposed on uranium production by the existing deployment cost. This cost floor exists because a significant portion of the deployment costs, notably ship operation, f maintenance and personnel expenses, are incurred each time the adsorbent is brought to the mooring site, emplaced, and then later winched up and brought to shore for elution, or processed on a vessel. The extent to which these expenses influence the final uranium production cost will be explored in more detail in section 3.4 and can be seen in Figure 9.

A previous publication [3] conducted an independent economic analysis of the WUSABI design as described by [32] so that this mooring and deployment strategy could be incorporated to the robust existing cost model, which consistently updates to reflect progress made in adsorbent technology. That work illuminated major cost drivers, most notably identifying the required chemical storage tanks and ships as making up a substantial portion of the deployment cost. Therefore, this work considers design changes to reduce these costs, as well as provide greater transparency to the higher fidelity economic analysis that is used with the current cost model. Significant design developments carried out here address the material of the storage tank by substituting a more cost effective alternative. Tank size was also manipulated to find the optimal frequency of turbine servicing, which affects not only tank but also service fleet size.

This paper will initially provide background on the cost-analysis of the current braid deployment system described above, which will serve as a base case. To achieve this, a recent cost analysis publication [7] will be referenced to highlight major cost drivers (e.g., adsorbent fabrication and performance) beyond deployment which affect uranium production costs. Then the symbiotic design, as adapted from [32], is presented in sufficient detail to conduct a cost-analysis of a refined WUSABI strategy. The lifecycle cost of a unit mass of adsorbent moored by WUSABI will be calculated with additional details considering the improvements made here. Finally, the results of various design sensitivities and optimizations of WUSABI parameters are explored.

2.1. Methodology

The methodology for this cost estimation has been applied to several variants of the technology [9, 6, 35, 34, 5] and uses discounted cash flow analysis to track the lifecycle cost of a unit mass of adsorbent. Input cost data used in this analysis comes from the most recently published cost analysis [6] of the ORNL adsorbents and the original description of the WUSABI design [32] unless otherwise noted. All costs presented are in 2016 dollars.

2.2. Reference Kelp-Field Deployment

The recovery process analyzed in recent publications will serve as the baseline to which the design proposed here will be compared and is thus described first. The deployment strategy consists of rows of adsorbent moored to the ocean floor in a kelp-field like structure. Polymer rope is interlaced with metal chains to prevent the net buoyant braids from floating to the surface or being dragged away by ocean currents. Work boats continually service the field, winching up adsorbent to transport it to a site where chemical processing and regeneration of adsorbent takes place. Previous publications found that deployment costs were reduced if the adsorbent field were supported by a centrally located mothership, so that only a single supply ship (as opposed to potentially dozens of work boats) must voyage to and from shore [38, 34]. Post elution the work boats again deploy the adsorbent and the process is repeated. Given its ubiquity in previous cost analyses, this will serve as the base case to which the WUSABI deployment strategy will be compared.

The cost of seawater uranium is constantly changing as the chemistry and recovery process are under continued development. Therefore, given uncertainties in adsorbent performance when exposed to a true marine environment, recovery cost is presented as a range rather than a single point. This reference scenario, used in previous publications [7, 8], attempts to provide the best and worst case scenario associated with the current technology, and will be summarized next along with the associated assumptions.

Experimentation by PNNL [31] has shown that biofouling, the growth of microorganisms in an ocean environment, may hamper the adsorbent's ability to take up uranium by up to 30%, when warm unfiltered seawater flows past an adsorbent sample in the presence of strong light. It remains unclear whether full or partial mitigation of oceanic biofouling may be achieved, or whether the fouling will persist in any ultimately selected deployment environment. Therefore, in this scenario the effects of biofouling will be considered as negligible in the best case and a 30% loss in uptake as the worst case.

A range of possibilities similarly exist for the rate of degradation suffered by the adsorbent upon its reuse. Early experimental data suggested that upon reuse the adsorbent would consistently suffer a 5% loss in uptake ability [38]. More recent experimental data, however, has suggested that the adsorbent degradation rate is dominated by exposure to seawater rather than the currently utilized mild elution chemicals [25]. The recovery of adsorbent capacity as a function of cumulative days of seawater exposure from all cycles of a unit mass of adsorbent over its lifetime can be seen in Figure 1. This model reflects the observations by PNNL that while capacity decreases with increased seawater exposure regardless of individual cycle length, below a threshold of 56 cumulative days adsorbent degradation is negligible. This time dependent model for degradation will thus serve as the upper bound while the flat 5% loss in uptake will provide the lower bound.

The governing parameters for the reference scenario can be seen in Table 1. The length of soaking campaign and number of adsorbent uses are determined using an optimization procedure [6] to find the lowest possible uranium production cost for the given set of inputs.

A cost breakdown is provided in Figure 2 showing the cost attributed to the three major process steps for the best and worst case. After adsorbent production, the mooring and deployment cost is the most significant contributor; reducing this cost by means of the novel WUSABI system presented here can thus have a substantial effect on the final uranium production cost. Additionally, significant reduction of the mooring and deployment cost could allow for a much greater number of optimized uses, further improving ura-

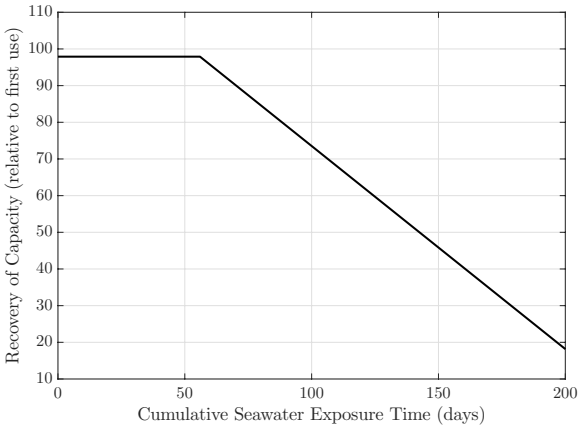

Figure 1: Loss in adsorbent uptake as a function of campaign length for the worst case degradation scenario, taken from [8].

Table 1: Governing Parameters for Reference Scenario

	Parameter	Best Case	Worst Case
Input Data	Temperature (°C)	20	
	Degree of Grafting (%)	250	
	Alkaline Solution	NaOH	
	Biofouling (% loss in uptake)	0	30
	Degradation (% loss per re-use)	5	Worst Case
Optimized Deployment Parameters	Number of Uses	17	13
	Length of Exposure Cycle (days)	46	12
Results	Uranium Production Cost	$460/kg U	$840/kg U

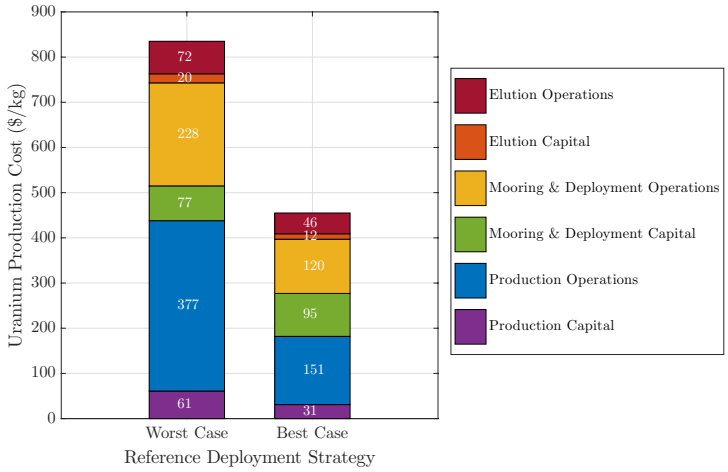

Figure 2: Cost breakdown for best and worst case scenario applied to the reference deployment strategy.

nium costs. Deployment and mooring costs are seen to comprise 40-46% of the estimated uranium production cost, so a transformative redesign of the deployment system has the potential to substantially ameliorate the cost of seawater uranium recovery.

2.3. WUSABI Deployment and Modifications

In an effort to substantially reduce the energy costs associated with operating the ships as well as fabricating the ships and mooring system, [32] proposed a system which autonomously and continuously takes the adsorbent from the ocean, through an elution process, and returns it to the ocean allowing control over the harvest period. The system is designed to function attached to offshore wind turbine structures, thereby eliminating the

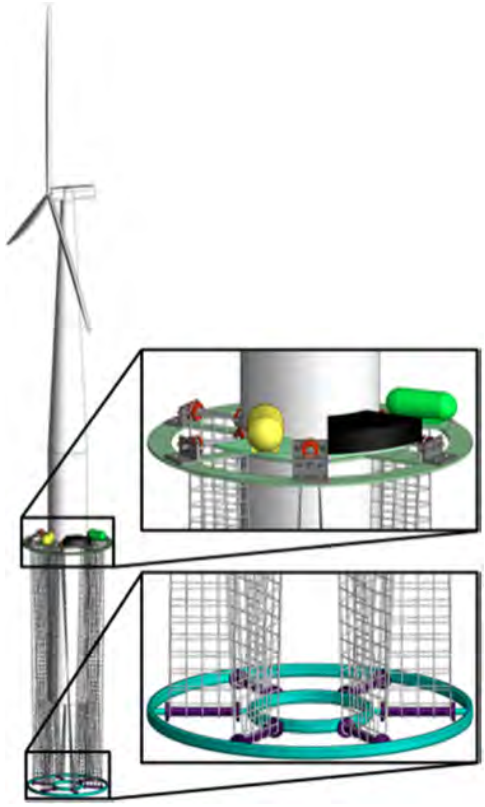

Figure 3: Three-dimensional view of continuous uranium recovery system with adsorbent belt looped around the turbine mast proposed by [32]. The elution plant is housed on the upper platform out of the seawater.

offshore mooring cost while also increasing the effective energy output of the wind farm.

Figure 3 shows the concept developed by [32] in which a platform at the base of the wind tower supports a belt of adsorbent that loops in and out of the water. The belt slowly cycles through the seawater beneath the tower and through an elution plant located on the platform. The belt is weighted in the seawater by rollers which also space out the loops and prevent the belt from tangling. Figure 4 shows the generalized system diagram showing the inputs, major components, and outputs of a symbiotic uranium harvesting system. Figure 5 depicts in more detail the autonomous elution and regeneration process of polymer adsorbent, described in [25, 30], as applied in a symbiotic uranium harvesting system.

The proposed system used 4 km of polymer rope adsorbent per system

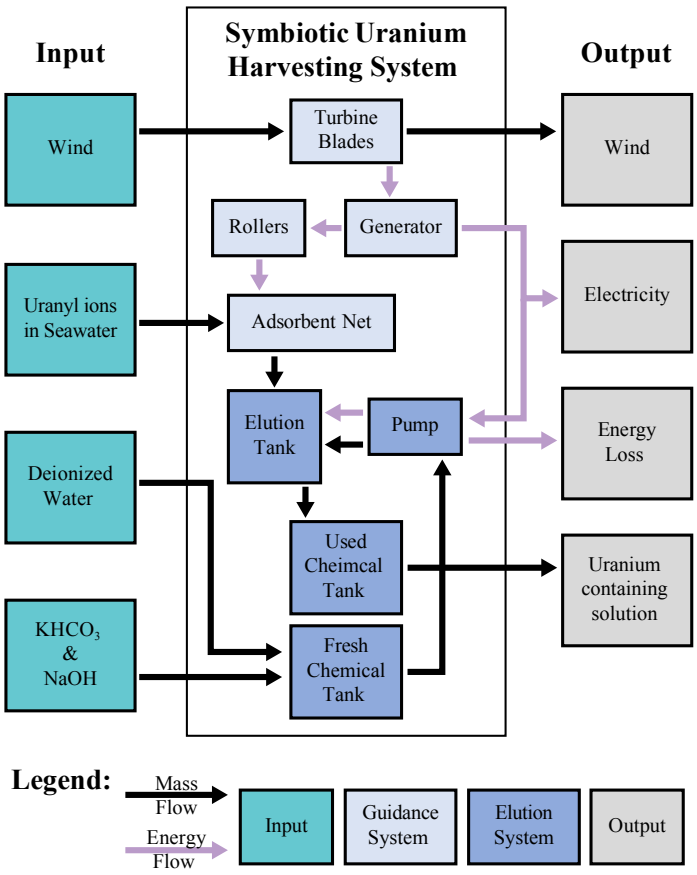

Figure 4: System diagram of symbiotic uranium harvesting system, such as that described by [32], showing inputs, major components, and outputs.

attached to an offshore wind turbine, and would yield 1.2 tonnes of yellowcake uranium per year. This is a sufficient amount to provide a nuclear power plant with fuel to continually generate 5 MW of electric power. Preliminary analysis conducted by [32] on the adsorbent belt and structural design to determine the first order scaling laws for this concept indicate that such a system is technically feasible. This paper seeks to do an independent cost-analysis for the continuous uranium recovery system proposed by [32], while also updating the design by targeting previously identified cost drivers. The cost analysis will be similar to that completed by [35] for the original reference deployment strategy.

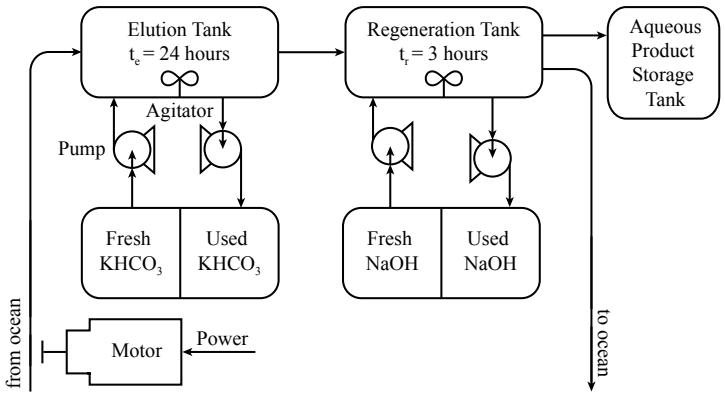

Figure 5: Diagram describing the autonomous elution and regeneration process of polymer adsorbent in a symbiotic uranium harvesting system.

The original design proposed by [32] was improved to provide sufficient capacity to store all required chemicals, while also considering trade-offs between storage tank capacity and servicing frequency. Each elution tank is constrained to be sized to contain a length of adsorbent polymer for the duration of the elution process, 24 hours, with the downstream regeneration tank sized so that the same belt speed allows the length of the adsorbent polymer to remain contained in the tank for the duration of the regeneration process [25, 30]. Finally, storage tanks were sized to contain enough of each chemical to sustain the system between service visits by work boats, which in the original publication by [32] was set to be the length of a single campaign of 38 days. In this publication, the time between service visits by workboats and the campaign length are two independent dynamic variables, on the order of days, optimized for the user-specified parameters.

With these design modifications, the continuous uranium harvester would be comprised of an upper platform constructed of beams radiating 16 m from the edge of the turbine and contain 20 rollers which loop the adsorbent belt in and out of the ocean. A similar platform is attached to the bottom of the turbine 100 meters below the surface with 20 weighted rollers to guide the adsorbent belt and prevent tangling even in the presence of strong currents. The upper platform is also supported with diagonal cables connecting the periphery of the platform to the turbine structure. Moreover, the adsorbent belt is reinforced with support ropes on either side (shown by the thick lines Figure 6). All calculations for the sizing and materials of the platform support cables, the adsorbent support ropes, as well as the upper and lower platforms themselves follow the design analysis of [32].

3. Cost Analysis of WUSABI Deployment strategy

In addition to updating the original design by [32] to reflect progress made in the recovery process, this work implemented additional changes aimed at improving the economics of the WUSABI strategy. This section will calculate the unit cost of uranium recovered, ($/kg U) using the updated symbiotic system, with the focus on the deployment infrastructure. Following the methodology used in the previous cost estimates [35, 6], the unit capital and operating cost associated with the three major process steps (adsorbent production, mooring and deployment, and elution) are calculated individually so they may be summed over all adsorbent deployments, N_{deploy}, using the time value of money to arrive at the adsorbent lifecycle cost according to the generalized equation below,

$$C_{\text{U}} = \frac{C_{\text{ads prod}} + C_{\text{mooring and deployment}} + C_{\text{elution and purification}}}{N_{\text{deploy}} U_{\text{uptake}}} \tag{1}$$

where C_{U}, $C_{\text{ads prod}}$, $C_{\text{elution and purification}}$, and $C_{\text{mooring and deployment}}$ are the unit costs of the uranium recovered, adsorbent production, elution and purification, and mooring and deployment, respectively, N_{deploy} is the number of adsorbent deployments, and U_{uptake} is the adsorbent capacity of the polymer.

Aside from ancillary changes resulting from the use of the WUSABI strategy, which are identified in the text below, the adsorbent production and uranium purification costs, $C_{\text{ads prod}}$ and $C_{\text{elution and purification}}$ respectively ($/tonne adsorbent produced), are calculated in the same way as the base case discussed previously, detailed in Table 1. Therefore, this section will primarily detail the cost calculation of the improved symbiotic mooring and deployment infrastructure, $C_{\text{mooring and deployment}}$ with more attention paid to the design perturbations unique to this work. The cost for a single symbiotic harvester is determined to find the total cost for a windfarm consisting of 100 offshore wind turbine-based systems, recovering a total of 1,200 tonnes of uranium annually, analogous to the reference kelp-field estimates. Calculation data using a representative set of adsorbent performance parameters, namely constant 5% per reuse degradation rate and a 30% loss in uptake due to biofouling, is presented in the Appendix.

3.1. Adsorbent Production Cost

The adsorbent production process for WUSABI differs from the reference case in a very important way. Rather than being deployed as individual

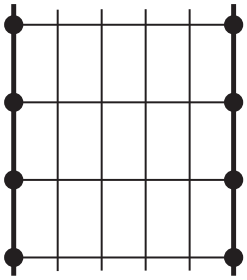

Figure 6: Adsorbent net used in the design by [32]. High-strength cable is represented by thick lines and adsorbent braids are represented by thin lines. For this section, $b_{\text{parallel}} = 4$ and $b_{\text{node}} = 2$ for use in (2).

braids, the adsorbent braids are fabricated into long narrow nets resembling rope ladders to traverse the underwater mooring system. Therefore, an additional cost is incurred to account for materials and fabrication expenses, but system robustness, resistance to tangling, is substantially increased.

The additional material required to sustain the shape of the net consists of structural wire incorporated into the adsorbent braids. Following the original system design by [32], the length of support wire required per unit mass of adsorbent is simply the inverse of the adsorbent linear density, λ_{ads} (kg/m).

The fabrication cost is a function of the width of the net, as measured by the number of braids fitting in parallel across the net, b_{parallel}, and number of braids per node in the net, b_{node}; in the case of the 2-D net used in this system, as shown in Figure 6, the number of braids per node is fixed at 2. The calculation for length of net construction, l_{net} (meters/kg), required per kg of adsorbent fabricated can be seen in (2):

$$l_{\text{net}} = \left(\frac{1}{\lambda_{\text{ads}}}\right)\left(\frac{1}{b_{\text{parallel}}}\right)\left(\frac{1}{b_{\text{nodes}}}\right). \tag{2}$$

The unit costs for both the material and fabrication come from those stated in the original [32] design and can be seen in Table 9 of the Appendix, along with the calculated cost per tonne of adsorbent.

3.2. Mooring and Deployment Cost

Relative to the conventional mooring strategy, WUSABI is more expensive to install and much less expensive to operate. This subsection identifies the capital and operating costs for WUSABI itself as well as costs associated with work boats and lease of the turbine platform. Costs for materials were

all taken from the original publication [32] of the design, adjusted to 2016 dollars, and can be seen in Table 3 of the Appendix. The cost to manufacture the end product from these materials was estimated as 50% of the material cost, as derived from [32]. Finally, an equipment installation and delivery cost equaling 39% of all equipment is used just as in the previous cost estimates [35].

3.2.1. Top Platform

The top platform is the primary structure, displayed in the top zoomed-in box of Figure 3, consisting of the support beams that hold all of the tanks along with the pulleys that move adsorbent around the system. This subsection will identify individual components of the top platform to provide calculations supporting the sizing of each deployment structure. The resulting numerical values for the overnight capital cost are tabulated in Table 5 of the Appendix.

The mass of steel required for the top platform, s_{top} (kg), is a function of the number of loops, n_{loops}, the length of the pulley shaft, l_{pulley}, (m) and the linear density of the beam, λ_{beam} (kg/m), and can be seen in (3):

$$s_{\text{top}} = (n_{\text{loops}} + 2\pi)\, l_{\text{pulley}} \lambda_{\text{beam}}. \tag{3}$$

A structural support cable is required to connect each pulley shaft to the mast of the turbine. The total length of cable required l_{cable} (m) depends on the angle between the turbine mast and beam, θ (rad), the length of the pulley shaft, and the number of loops (4).

$$l_{\text{cable}} = \frac{l_{\text{pulley}}}{\sin\theta} n_{\text{loops}}. \tag{4}$$

Lastly on the top platform, the cost of all elution and storage tanks is calculated. The volume, and thus cost, of each tank is a function of the mass of adsorbent on each platform along with adsorbent performance and other deployment parameters considered below. The elution and regeneration tanks are reaction tanks and must hold enough of a given solution to chemically treat the amount of adsorbent contained within it at any given time. Given that adsorbent is in constant motion through this system, these tanks must be supplied with top-up solution while used chemicals are removed in order to always supply adequate elution or regeneration conditions for the new segments of adsorbent net entering the tanks. Therefore, auxiliary chemical storage tanks are fitted with a moving membrane to enable the same tank to store the fresh and depleted chemical. The size of the

reaction tanks is a function of the chemical demands and exposure time for the respective process, which are given in Table 4 of the Appendix. The size of the storage tanks is also a function of the frequency with which they are serviced to replenish fresh chemicals and removed used supplies.

The initial cost estimate put forth by [32] assumed that ships serviced the wind turbines once a month to replenish consumed chemicals. Therefore, the tanks were sized to hold a 30 day supply of each chemical. Another aspect of the original design is tanks manufactured of 316 stainless steel; cost reduction efforts have led to a revised design featuring cross linked linear polyethylene (XDPE) tanks, which are resistant to chemical corrosion at low molarities [11, 20] such as used in the elution and regeneration process. A linear regression from vendor quotes is used to determine the cost of tanks as a function of volume, v (m^3), just as was done in the original cost estimate for stainless steel tanks. Equations (5) and (6) detail the resulting cost of tanks made out of XPDE, $Cost_{\text{XDPE}}$, and stainless steel, $Cost_{\text{ss}}$, respectively. Although the regression only consisted of data for tanks ranging from 0.568 to 51.7 m^3, a Poly Processing Company representative stated that for this application with dilute solutions no realistic limits exist on the maximum size of a tank made of XDPE.

$$Cost_{\text{XDPE}} = 513v + 1674 \tag{5}$$

$$Cost_{\text{ss}} = 163v + 69030 \tag{6}$$

Similarly, the elution and regeneration tank costs, (7), are a function of the required volume, v, and agitation power, P_{ag} (W) analogous to a land based system, and thus derived from previous cost analysis publication [35].

$$Cost_{\text{tank}} = Cost_{\text{XDPE or ss}} + (3365P_{\text{ag}}^{0.1732}). \tag{7}$$

The comparison of tank cost for stainless steel versus XDPE can be found in Table 4 of the Appendix for a representative case.

The stainless steelf tank costs are seen to scale more favorably with tank volume than the XDPE tanks, presumably due in part to the lower strength-to-weight ratio of XDPE. Except at the highest volumes, though, XDPE tanks prove to be lower cost. Hence, savings were realized by switching out most of the stainless steel tanks for XDPE. Under some adsorbent performance scenarios, the alkaline storage tank is an exception. Using XDPE in place of stainless steel on the remaining tanks propagates to a uranium production cost savings of 9%.

The best choice of tank material depends upon various parameters that influence the required tank volume, for instance the frequency with which the turbines are serviced by work boats. Therefore, the assumption that turbines would be serviced monthly was revisited at the same time as the tank design was reconsidered. Increasing the frequency of service will decrease the required volume and cost of the storage tanks but also increase the number and/or size of work boats required to service the field. The cost of each boat is determined using the empirical correlation employed in the kelp-field deployment strategy [39, 34] where the size, and thus cost, of each work boat is a function of the mass it must carry. Therefore, the number of ships required, service frequency, and tank volumes must be optimized subject to the constraints defined in this section to provide the lowest uranium production cost resulting from these competing feedbacks. In this work, the optimization is carried out by brute force since the constraints effectively act to reduce the number of independent variables to one (number of ships).

In moving away from the fixed monthly service assumption, though, it is first necessary to determine the time required to service each platform, t_{p}, to load and unload chemicals. Literature for a United States Department of Energy (DOE) study of wind farm economics [29] was examined to conclude that 8 hours at each platform is a fair but conservative estimate; for reference, the original publication assumed 1 day. It was also determined from data for these proposed wind farms that a typical ship would take 6 hours to travel to a servicing port and back, t_{travel}. An assumption was made that once the ship returns to shore, a 1 day turn-around time is required before it can return to sea with a new batch of chemicals. It is also assumed that each ship services an identical number of platforms, which is simply the quotient of the number of platforms in the field and number of ships, n_{ship}. These values were all used to find the time between platform service, t_{service}, in days as seen in (8).

$$t_{\mathrm{service}} = \frac{t_{\mathrm{p}} \frac{n_{\mathrm{p}}}{n_{\mathrm{ships}}} + t_{\mathrm{travel}}}{24 \text{ hours/day}} + 1 \text{ day at shore} \tag{8}$$

The time between services is then used to determine the volume of the tank, v. Table 4 in the Appendix provides the volume of each chemical required to elute a unit mass of adsorbent. In this data, taken from [30], if the required volume for any chemical is V_{chem} (m^3/kg), the size of its tank is determined from the total mass of adsorbent on the platform, m_{plat} (kg). The average number of times each kg of adsorbent is eluted between servicing visits is $\frac{t_{\mathrm{service}}}{t_i}$, for any given point in time, t_i. So the tank volume,

v_{tank}, is given by

$$v_{\text{tank}} = V_{\text{chem}} \left(\frac{t_{\text{service}}}{t_i} \right) m_{\text{plat}}. \tag{9}$$

Since choosing the number of ships uniquely specifies t_{service} and vice versa, the number of ships was treated as the independent variable and iterated to achieve the lowest possible uranium cost. Clearly increasing the number of ships decreases the time between services, allowing for smaller storage tanks. To determine at what point this decrease in storage tank cost is offset by the added ship cost, the final uranium production cost for an illustrative base case as a function of fleet size is pictured in Figure 7. The uranium production cost is seen to become very large as the number of ships is decreased. The modest economies of scale benefit from moving toward fewer, larger ships is more than offset by the cost of tanks storing very large volumes of chemicals.

The cost model automatically optimizes the number of ships in response to any change in input design or adsorbent performance parameters. The integer constraint on the number of ships results in the jagged nature of the uranium production cost seen in Figure 7; it is important to note, however, that these fluctuations are only on the order of a few dollars. This contrasts the original design, which determined the number of ships based on the assumption that each ship would service 30 turbines over the course of a month. The optimal strategy for the reference case called for a bigger fleet of smaller ships with a servicing interval of 5.4 days, resulting in a nearly 30% uranium production cost savings.

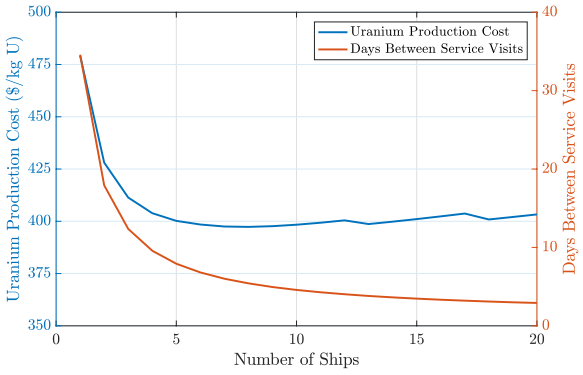

Figure 7: Uranium production cost as a function of number of ships in fleet for a 1,200 tonnes U/year field.

All of the costs attributed to the top platform for a single harvester unit corresponding to the representative case can be seen in Table 5 of the Appendix. The total cost for the top platform, along with all other structural components, for the field can be found in Table 7.

3.2.2. Bottom Platform

The bottom platform, shown in more detail in the bottom zoomed-in section of Figure 3, is a structural steel frame with HDPE rollers allowing adsorbent to be moved by the pulleys on the upper shaft. The mass of steel required to construct the cylindrical base frame, m_{base} (kg), is a function of the total length of the frame, l_{base} (m) , the inner and outer diameter of the rollers, r_{inner} and r_{outer} (m) respectively, and the density of structural steel, ρ_{ss} as seen in (10):

$$s_{\text{base}} = l_{\text{base}}\pi \left(\left(\frac{r_{outer}}{2} \right)^2 - \left(\frac{r_{inner}}{2} \right)^2 \right) . \rho_{\text{ss}} \tag{10}$$

The total length of the frame, given by (11), is a function of the circumference of the inner and outer foundation rings, as calculated by their diameters, f_{inner} and f_{outer} and the pulley shaft required for each loop. A diagram of this frame is shown in Figure 8.

$$l_{\text{base}} = f_{\text{inner}}\pi + f_{\text{outer}}\pi + l_{\text{pulley}} n_{\text{loops}} \tag{11}$$

The capital expense for the bottom platform is a function of its mass and can be found in Table 6.

3.2.3. Adsorbent Net

Running between the two platforms is rope providing support to the adsorbent net. Since this support rope runs along each side of the adsorbent net up and down each loop (depicted by the thick lines in Figure 6), the total length of rope required for each harvester, l_{rope} (m), is simply a function of the number and length of loops (i.e. the distance between the upper and lower platforms), l_{loop} (m) as shown in (12). This formulation is used in combination with the cost of the adsorbent support rope taken from [32] to arrive at the total belt cost seen in Table 7.

$$l_{\text{rope}} = 4 l_{\text{loop}} n_{\text{loops}} \tag{12}$$

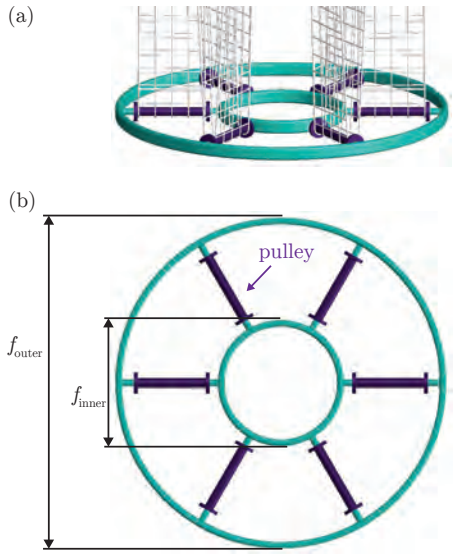

Figure 8: Bottom platform frame (a) as shown in the zoomed-in section of Figure 3 and (b) top down view. The inner frame and outer frames have diameters of f_{inner} and f_{outer} respectively. The pulleys that guide the adsorbent net are shown in purple. In this diagram, the number of loops of the net, $n_{\text{loops}} = 6$ for use in Eq (11).

3.2.4. Fee Paid to Wind Turbine Owner

The final cost component of the harvester capital cost is the fee paid for use of the wind turbine as a mooring platform. This fee is modeled as payment of a part of the turbine capital cost by the operator of the uranium recovery system. Hence the cost, fee, calculated in (13), is proportional to the electricity use of the harvester system, $e_{\text{harvester}}$, as compared to the capacity of the turbine; the power demand to simply propel the adsorbent net and stir the tanks is on the order of 0.1% of each 5 MW rated turbine. The capital cost of the turbine, cap_{turbine}, and electricity production, e_{turbine}, both come from the DOE economic analysis of offshore wind markets [29].

$$fee = \frac{e_{\text{harvester}}}{e_{\text{turbine}}} cap_{\text{turbine}} \tag{13}$$

In addition to the agitation power required for each of the tanks, electricity is also required to keep the adsorbent in constant motion. The 820 W stated by [32] is used along with the system uptime, sys_{up}, to determine the annual electricity consumption of the harvester.

$$e_{\text{harvester}} = (820 + 2P_{\text{ag}})\, sys_{\text{up}}\, (24 \times 365) \tag{14}$$

An alternate approach would have been to model the fee as an operating expense, presumably also in proportion to the uranium recovery system's electricity consumption. As this would have required assumptions regarding the value negotiated for that electricity at its point of production, it was decided to take the conservative route of treating the fee as a one-time capital expense.

3.2.5. Servicing Fleet

In addition to all of the harvester units, the total field capital cost includes the cost of purchasing the ships required for service. Ship capital cost is calculated using the same methodology as in the kelp-field deployment strategy [39, 34] where ship cost is a function of size dictated by the required chemical capacity. The cost of all ships and all other components of the capital cost for the entire field can be found in Table 7 for the illustrative case. In the approach taken here, ship costs benefit modestly from economies of scale, so that a doubling of ship deadweight tonnage results in an increase of only 70% in its capital cost. All of these costs are summed to find the capital cost of each harvester unit and the entire field.

3.2.6. Operating Cost

Given the autonomy of WUSABI, there are few operating cost elements: only the labor and fuel required for the work boats are itemized. The operating costs for these expenses are calculated in the same way as for the kelp-field deployment [34].

The ships are sized based upon their maximum required cargo capacity. Ships carry bicarbonate, alkaline solution, and product solution and are sized to be able to carry their maximum payload of each at the same time. The fuel consumption calculations, however, recognize that on average they carry only half of their product payload. The calculated annual operating costs and number of ships required for the intermediary case can be seen in Table 8 of the Appendix.

3.3. Elution Cost

The elution and purification cost calculations remain mostly unchanged from previous economic publications. While the cost is partly decreased due to the off-shore migration of adsorbent elution taking place on the platform, there remain subsequent purification processes that continue to take place on land. The costs associated with processes encountered after the bicarbonate elution are calculated using the same methodology as previous cost analysis [6, 35].

3.4. Lifecycle Unit Cost

Next, the uranium production cost resulting from the use of the current adsorbent with the WUSABI strategy is compared against that of the kelp strategy (Table 2). The best and worst case adsorbent performance parameters, a function of degradation and biofouling, applied to the kelp-field deployment strategy are analogously applied to the WUSABI strategy. The WUSABI uranium production cost is similarly optimized [6] to determine the lowest achievable cost by varying the length of soaking campaign and number of adsorbent uses. It is clear that coupling the recovery of seawater uranium to off-shore wind turbines can result in a ca. 60% reduction in mooring and deployment cost. This propagates to significant savings in the seawater uranium production cost as a nearly 32% savings can be achieved if the best case scenario regarding adsorbent performance can be realized.

Table 2: Final uranium production cost, and associated deployment parameters, for both the reference kelp-field and WUSABI strategy for the bounding adsorbent performance parameters.

		Kelp-Field	**WUSABI**
Worst Case	Uses	13	19
	Days	12	10
	Cost per kg U	$840	$640
Best Case	Uses	17	20
	Days	46	57
	Cost per kg U	$460	$401

Figure 9 breaks down the contribution of each deployment expense to the uranium production cost for both the reference kelp-field and WUSABI strategy; to analyze the cost impact of the WUSABI system adsorbent related costs are not included as the same adsorbent type is used in both systems. The majority of benefits derived from utilization of the WUSABI strategy can clearly be attributed to the reduction of labor costs under WUSABI. Use of an existing structure also circumvents the requirement of mooring by chains and ropes, which are notably costly in comparison to the analogous structural members in WUSABI, the top and bottom frames.

Aside from the reduction in mooring capital and operating costs, adoption of the WUSABI mooring system allows for a shift to more favorable deployment parameters. Since the cost of each mooring and deployment event is lower, it becomes cost effective to pursue a greater number of adsorbent recycles. It is worth mentioning that the true optimal number of uses for the WUSABI strategy may actually exceed 20, but due to lack of

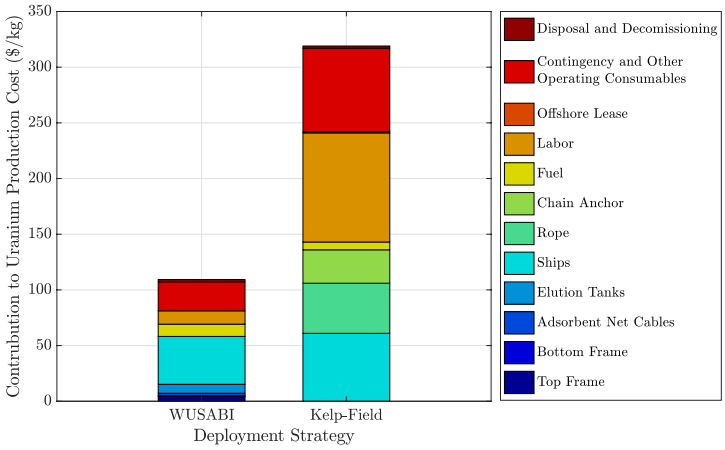

Figure 9: Cost breakdown of capital and operating costs for both deployment strategies for the representative intermediary adsorbent performance case. Given that identical adsorbent types are used in both deployment strategies, adsorbent related costs are not depicted.

experimental data in that range, an upper bound of 20 uses is imposed. Similarly, longer soaking campaigns can be endured, allowing for greater uranium recovery from a single unit mass of adsorbent. A lower mooring capital cost favors a larger field with longer soaking times, rather than a smaller one with a greater turn-over rate.

4. Sensitivity Analyses and Design Perturbations

In an effort to further reduce the cost of uranium recovered using WUSABI, sensitivity analyses are used to identify major cost drivers in this updated strategy. The following section will explore how hypothetical design perturbations affect the final uranium production cost.

4.1. Sensitivity to Number of Loops

Following the design put forth in the original publication, each harvester unit is constructed with 20 loops, so that the adsorbent travels down then up the height of the system 20 times between passes through the elution and regeneration reaction tanks. Given a fixed number of loops per platform, the mass of adsorbent required per platform m_{plat}(tonnes), to meet the annual uranium recovery requirement, U_{annual} (tonnes), scales the required radius of the platform and loops. This mass required per platform is a function

of lifetime adsorbent uptake, U_{lifetime} (kg U/tonne ads), the number of deployments experienced by each unit mass of adsorbent, N (deployments), length of soaking campaign, t_c (days), and the fixed number of platforms in the field, n_{plat} as seen in (15)

$$m_{\text{plat}} = \frac{U_{\text{annual}}}{U_{\text{lifetime}}} N t_c \left(\frac{1 \text{ year}}{365 \text{ days}} \right) \frac{1}{n_{\text{plat}}}. \tag{15}$$

A greater number of loops decreases the strength required of each pulley, and consequently the associated material cost. Contrastingly, having fewer, wider loops increases the overall footprint of the harvester unit, increasing the cost of constructing the base frame, which is a function of diameter. These trade-offs were shown in section 3.2.1 and 3.2.2 to affect the mass of structural steel required according to (3) and (10) for the top and bottom platforms, respectively. The material and installation cost associated with the structural steel frames (including costs associated with painting the structural steel and mounting sacrificial anodes for prevention against corrosion) and loop shafts constitute ca. 20% of the mooring capital cost, a nontrivial contribution. The final uranium production cost for the best and worst case performance parameters as a function of number of loops can be seen in Figure 10. Stars in this figure indicate the optimized value for both cases.

Given the small contribution of the mooring and deployment capital to the final uranium production cost, and more specifically the cost associated with the support frame, little impact is felt on the uranium production

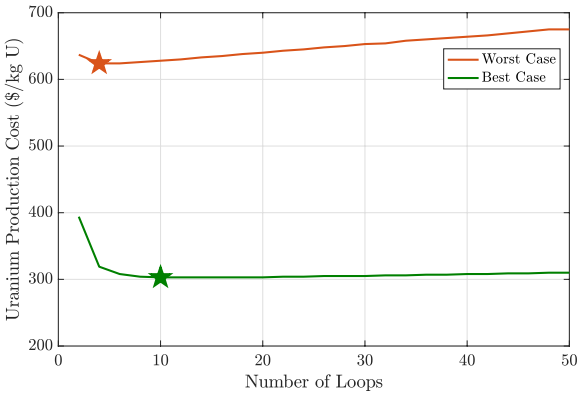

Figure 10: Uranium production cost as a function of number of loops on each harvester unit for the worst (orange line) and best (green line) cases. Stars indicate the optimized value for both cases.

cost by optimizing this aspect of the design, as noted by the very shallow minimum in Figure 10. There is an exception however, in both adsorbent performance cases, at very small number of loops which would require prohibitively large frames in order to support enough adsorbent to acquire 1,200 tonnes/year of uranium needed to supply a 5 GW nuclear power plant. Therefore, any external restriction forcing the number of loops to be small would not be served best by a system of this design and it is outside the scope of this paper to construct alternative designs for such a scenario.

The best case adsorbent performance scenario favors a greater number of loops due its longer campaign lengths. The reduction in the average amount of uranium recovered by each adsorbent per unit time, which accompanies longer campaign lengths, requires that more adsorbent be in the water at any given time to meet the 1,200 tonne requirement. As the field size increases, the mass of adsorbent required by each platform increases, assuming the number of turbines is constant. Eventually the cost of an additional loop becomes more favorable than the cost associated with increasing the diameter of the entire frame.

4.2. Sensitivity to Number of Turbines in Field

The size of the wind farm is also a design parameter worth exploring. A smaller field requires a smaller servicing fleet, and as was pointed out earlier, the capital and operating cost attributed to ships makes a nontrivial contribution to the final uranium production cost. The competing feedback is that each harvesting structure must be larger to support a greater mass of adsorbent, resulting in fewer but more expensive structures. In the original publication of this design, the size of the field was selected using a wind generation requirement of 5 GW. In the updated design referenced here, 100 turbines was selected as it was assumed to represent a realistic possibility. The plot in Figure 11 shows the sensitivity to final uranium production cost as a function of number of turbines. Stars in this figure indicate the optimized value for both cases.

Both adsorbent performance cases can be characterized by an optimal number of turbines less than the referenced 100, but closer to 30. In both cases this is due to the significant cost of the servicing fleet, as shown earlier in Figure 9, as compared to the small contribution from the structural costs. The inherent trade-offs between constructing fewer, larger versus a greater number of smaller turbines is far out-shadowed by the cost savings achieved by reducing the time required to visit all platforms, and thus the size of the service fleet. The time to service each platform is conservatively estimated at 8 hours, regardless of adsorbent performance, meaning time to service any

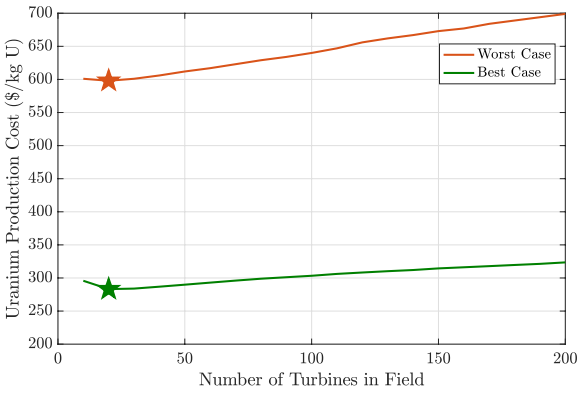

Figure 11: Uranium production cost a function of field size for the worst (orange line) and best (green line) cases. Stars indicate the optimized value for both cases.

given size field does not deviate between cases [29]. Therefore, differences between fleet costs across adsorbent performance cases are dominated by chemical storage requirements with regards to ship size, resulting in a similar optimized field size for both the best and worst case scenario. At very large field sizes the trend is increasingly evident in the less desirable adsorbent performance scenario, which assumes that adsorbent degradation increases with immersion time and thus favors shorter campaign lengths. The higher turn-over rate in this worst case scenario requires more ships and therefore sees greater savings by decreasing the number of turbines each ship must visit.

The sensitivity of final uranium production cost to this parameter is especially important given the uncertainty and lack of selection ability regarding the number of platforms in any given field. Since the first commercial offshore wind farm in the United States began operation only recently in 2016 with only five structures, there is little data to be analyzed to find a representative value for a system that would be employed domestically. In addition, if seawater uranium via WUSABI were to supply all of the current 60,000 tonne U/year world annual uranium requirements, given the current state of the best case adsorbent technology, approximately 5,000 turbines would be needed. It is likely to be some time before this many are available, but seawater uranium is not anticipated to become a critical source of uranium supply for some decades, while offshore wind power is expected to rapidly advance.

The resulting cost impact of both of these sensitivity analyses can be seen in Figure 12, which depicts the difference in final uranium production

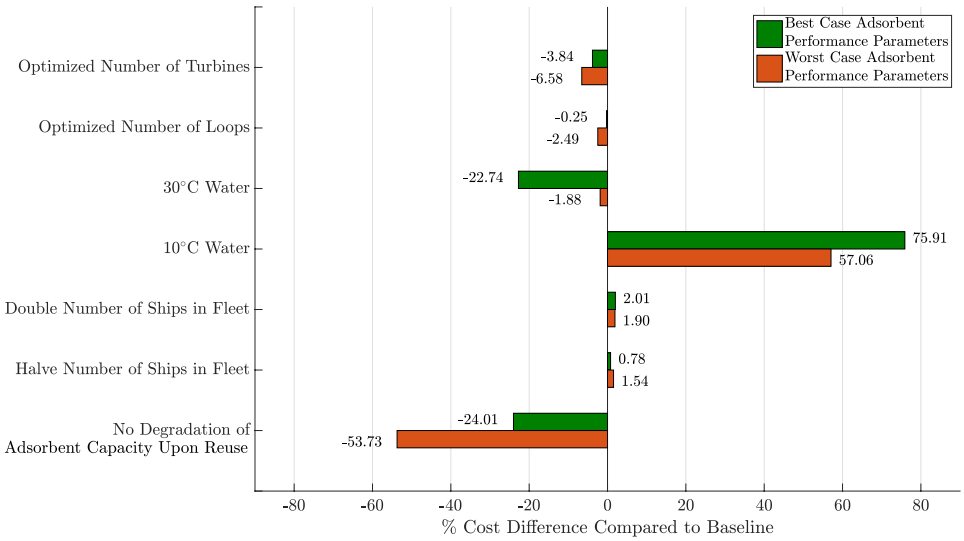

Figure 12: Percent change in uranium production cost for several hypothetical design and adsorbent performance scenarios.

cost of applying these design changes, using the optimized values indicated by the stars in Figures 10 and 11, as compared to the baseline uranium production costs for the WUSABI implementation described in Table 2. This demonstrates that further cost reduction can be achieved by continuing to improve the design, further supporting the use of the WUSABI scheme over the traditional kelp field-like structure. To give context to these areas of potential savings, the cost impacts of several other hypothetical design or adsorbent perturbations are also shown in Figure 12. It is clear from this figure that factors affecting the total adsorbent lifetime capacity, such as water temperature (to be discussed in the next section), and degradation upon reuse have the steepest impact on uranium production cost. While the WUSABI system discussed here does not directly affect adsorbent capacity, the lower cost per deployment event, as shown in Figure 9, results in a greater number of economical recycles, ultimately increasing the lifetime capacity of each unit mass of adsorbent.

4.3. Depth Dependent Temperature Profiles

The reference case models uptake as if all braids are exposed to a single uniform ocean temperature. Depending on the height of the turbine and the specific deployment location however this may not be representative of reality. This could have a significant influence on final uranium production

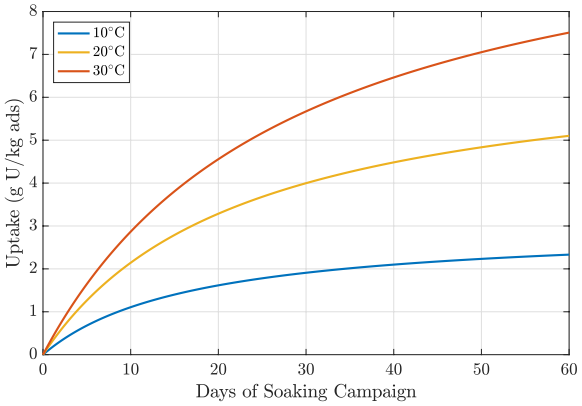

Figure 13: Temperature dependence of adsorbent performance as a function of length of soaking campaign, as calculated using the model first described in [6] and updated based on data published in [24, 37, 26].

cost because previous experimentation by PNNL has shown that uranium uptake increases nearly linearly with water temperature [24, 37, 26]. Figure 13 depicts the effect of temperature on time dependent adsorbent uptake. Therefore, the following section investigates the effects of marine temperature gradients and incorporates them into the uptake model to find ideal turbine height.

It is clear from Figure 13 that in addition to just temperature, the point in time along a soaking campaign a given temperature is experienced by an adsorbent is important. Due to the steepness of the initial slope, an adsorbent exposed to warmer water at the beginning of its lifetime will result in a higher uptake than an analogous adsorbent moving from cold to warm waters.

Time steps of one day are used to track the depth of a representative unit mass of adsorbent over its entire length of campaign, t_c. Each adsorbent is assumed to travel the same path, which is dependent upon the height of the turbine and the number of loops.

Each iteration uses the time, t, and temperature, T, dependent one-site ligand saturation model for uptake, U, to find the incremental uptake for that time step. The one-site ligand saturation model, used in all previous cost analyses [35, 5, 6] is a function of the temperature dependent saturation capacity, $\beta_{\max}$, and half saturation time, K_D, and is shown in (16)

$$U(t,T) = \frac{\beta_{\max}(T)t}{K_D(T) + t}. \tag{16}$$

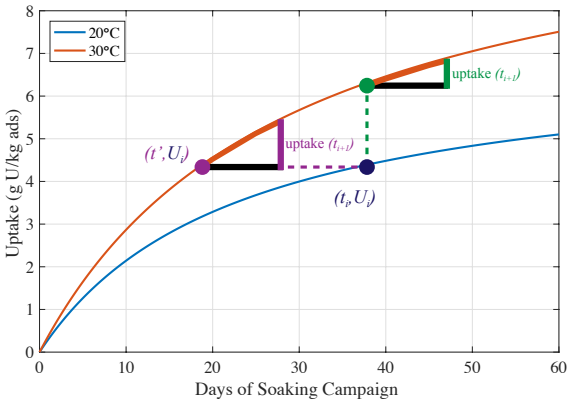

Figure 14: Illustration of the method for determining incremental uptake as a unit mass of adsorbent moves through water of different temperatures, as shown for a hypothetical case.

At any given point, t_i, during an adsorbent's campaign the uptake of the next time step, t_{i+1} can be calculated in two different ways: the position along the temperature dependent uptake curve experienced by t_{i+1} can be determined using the current time step, t_i, or uptake, U. Extrapolation along the time or uptake axis can be used to calculate either the corresponding uptake or time, t'. These two possible methods are illustrated in Figure 14 for a hypothetical unit mass of adsorbent moving from 20°C to 30°C water.

It is assumed that subsequent uptake performance will be dependent upon the progress made toward saturation, therefore interpolation along the x-axis is believed to be more reflective of reality. The current uptake is used to determine the effective immersion time at this new temperature, t' as seen in (17)

$$t' = \frac{K_{\mathrm{D}} U_i}{U_i - \beta_{\max}(T)}. \tag{17}$$

The incremental uptake experienced over the new time point is then simply calculated by moving along the current temperature dependent uptake curve, as depicted by the purple line in Figure 14. Although the time of soaking at each temperature, Δt, is the same, these two methods result in different incremental uptakes, as seen by the height of the respective lines. The marginal uptake at each time step is iteratively summed to arrive at the total uptake achieved by an adsorbent over the entire length of campaign as seen in (18). It is evident in (18) that issues would arise when the uptake at the current temperature exceeds the saturation capacity of the subsequent

temperature. In these extreme cases the math would suggest that uranium may begin to desorb off of the braid. Due to a lack of empirical data suggesting a quantitative model for an unloading curve, any such situation is simply treated as having taken up 0 grams of uranium.

$$U_{t_{i+1}} = U\left(t', T_{t_i}\right) + max\left(0, U\left(t' + \Delta t, T_{t_{i+1}}\right) - U\left(t', T_{t_i}\right)\right). \tag{18}$$

Figure 15 shows the average annual temperature gradient recorded by the World Ocean Database for three potential deployment locations of this system [27]. From this plot it can already be concluded that the cold waters and steep temperature gradient of the California coast will not be the most economical location given the temperature dependence of adsorbent performance. The Gulf of Mexico and North East, however, offer more suitable conditions where there are competing feedbacks regarding the draft of the turbine.

Taller underwater platforms extending to greater ocean depths can support the same mass of adsorbent with a smaller footprint, potentially resulting in a lower construction cost. There exists a trade-off between the material requirements for a short platform with a wider radius as compared to a taller narrower one. The more dominant and interesting feedback, however, is the lower uptake achieved by the adsorbent net if it extends into deeper colder waters.

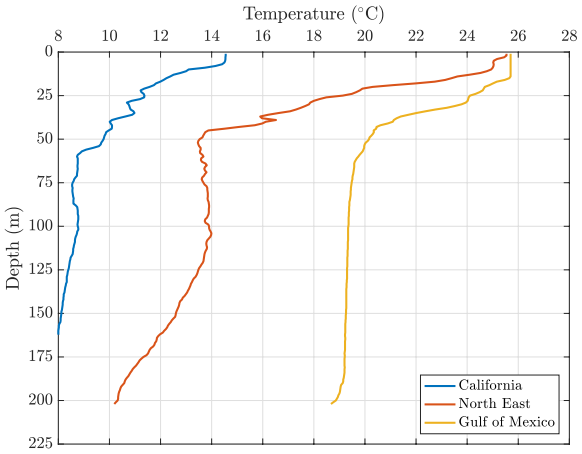

Figure 15: Marine temperature profiles for representative deployment sites. Average annual marine temperature gradient data used as recorded by the World Ocean Database [27].

The sensitivity of uranium production cost to adsorbent net depth (dictated by the draft of the offshore wind turbine) is shown in Figure 16 for both the best and worst case adsorbent performance scenarios for the two relevant deployment locations. Given the very trivial contribution the WUSABI structure makes to the final uranium production cost, as was discussed quantitatively in Figure 9, the optimal turbine height is primarily a function of the location dependent temperature gradient.

It is clear that the sharp drop-off in temperature characteristic of marine environments off the north eastern coast of the United States strongly favor shorter turbines that keep the entirety of the adsorbent net immersed in warmer waters. If the worst case adsorbent performance parameters are more indicative of reality, then there is significant economic benefit from the greater uptake offered by warmer water. This effect will be less pronounced if the best case adsorbent performance parameters are more indicative of reality because if the best case adsorbent performance parameters can be achieved and longer campaigns can be sustained to increase lifetime uranium recovery, the temperature effects are less dominant and the structural cost of varying turbine drafts becomes increasingly important.

The reason for this divergence in optimal turbine trend can be conceptualized by considering that the cost to produce a unit of adsorbent is nearly identical in these cases, only the resulting performance differs. The worst case scenario favors shorter campaign lengths due to the time dependence of adsorbent degradation. At these short soaking campaigns, uptake remains

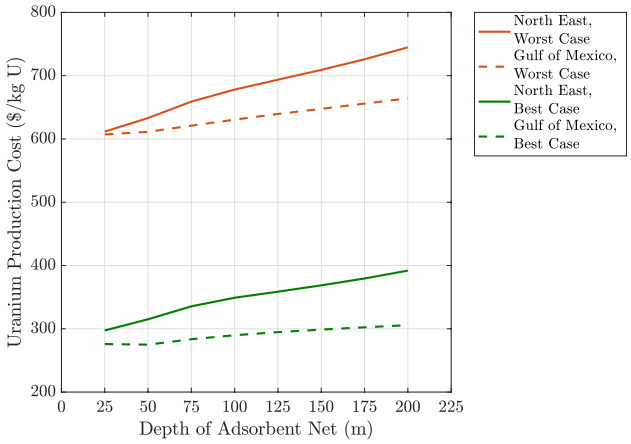

Figure 16: Sensitivity of uranium production cost to depth of adsorbent net (dictated by the draft of the offshore wind turbine) given the ocean temperature gradient for two representative deployment locations.

in the steep nearly linear portion of the one-site ligand saturation model, therefore marginal increases in temperature have a more significant payoff in terms of uptake as compared to adsorbents which closer approach saturation. The shorter structures offer these warmer waters, at the expense of a wider radius, allowing the adsorbent to recover more uranium and recoup the cost of adsorbent production, which is much larger, on a per unit of uranium basis, than that of the WUSABI structure. Therefore, in the case of short campaigns with comparatively low uptake, the incremental uranium recovered by exposure to warmer water is the driving factor in favoring the depth of the adsorbent net.

In the case of longer campaign lengths, which is typical of the best case adsorbent performance parameters scenario, a larger adsorbent field is required. Since the number of turbines is a fixed parameter, the attached uranium recovery infrastructure must increase. The small but increased structural cost associated with supporting more adsorbent begins to exert influence on the cost as the marginal increase in uptake offered by warmer waters becomes less important given that these adsorbents are nearing saturation capacity.

While the uranium complexation with amidoxime benefits from elevated temperatures, it is possible that a competing feedback of increased biofouling also exists in warmer waters. This possibility, and its effect on the cost of seawater uranium production, is not included in this analysis due to the lack of empirical data quantifying the relationship between temperature-accelerated biofouling and a decrease in uranium uptake. Previous work has used the temperature dependent heterotrophic bacterial growth as an initial means of scoping the economic effects of temperature enhanced biofouling [2]. More recent work [4, 23], however, have indicated that abiotic dissolved organic matter is a significant driver in the loss of adsorbent uptake, suggesting the previous method likely overestimates the negative feedback introduced by warmer waters and is thus not replicated here.

5. Conclusions

This work has detailed the updated cost model and progress made in reducing the cost associated with recovering uranium from seawater by symbiotically using offshore wind turbine structures as mooring and deployment structures. Basic updates were made to the original design to achieve compatibility with progress made regarding adsorbent performance and characteristics. Moreover, design and deployment elements were altered and

optimized to further improve economics. All of these changes resulted in a cost savings of over 30% as compared to the original kelp-field design.

Syncing deployment via the WUSABI strategy with an existing detailed cost model for adsorbent production and elution not only provides a more robust cost estimate, but also allows for continued design improvements such as those presented here. Unlike the cost analysis in the original publication, this economic model progresses in tandem with adsorbent technology. Therefore, as experimental data continues to be made available and evolutions in adsorbent performance are achieved, design and deployment parameters of the WUSABI strategy can continue to be optimized. Additionally the sensitivity analyses conducted highlight areas of potential future savings.

Additional cost sensitivities will investigate the placement of the adsorbent fibers deeper into the ocean and out of the photic zone, the location highest in biofouling activity, which will result in increased structure costs due to taller, narrower underwater platforms. While moving the fibers into deeper waters will likely reduce the amount of light penetration and hence biofouling activity to increase uranium uptake, it will also place them in colder waters, thereby acting to reduce the uranium uptake.

Recent work indicates that uranium-adsorbing materials with the optimal chemical properties for high adsorbent capacity have inherently low tensile strength and durability [43, 44, 46, 19]. This suggests that some adsorbent types would likely not be strong enough to be woven into a belt such as that utilized by [32] in this design. Therefore, work is underway to decouple the mechanical and chemical functional requirements of the proposed design by using a two-part system in which a hard permeable outer shell with sufficient mechanical strength and durability for use in an offshore environment and chemical resilience against elution treatments serves as the protective element for uranium adsorbent material with high adsorbent capacity in its interior, as shown in Figure 17 [17]. In theory, a device that utilizes such shell enclosures would be able to make use of adsorbents with greater uranium adsorption capacity than can be used in the kelp-field deployment, and hence would likely result in a decreased production cost of seawater uranium. Designs for uranium harvesting systems utilizing these shell enclosures are the topic of current research [14, 13, 15, 16, 18, 12] and their cost optimization will be the topic of a future study which builds upon the methods presented herein.

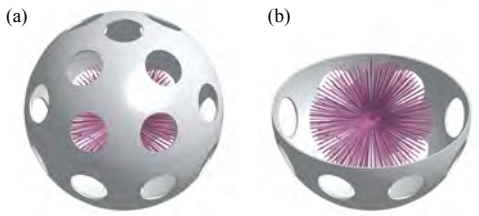

Figure 17: Initial adsorbent concept from [17] with decoupling of mechanical and chemical requirements. Soft, inner adsorbent sphere (shown in pink) is encased in tough, outer protective sphere (white). Outer sphere features holes to allow adequate seawater to adsorbent interior.

6. Acknowledgments

This work was supported by the U.S. Department of Energy Office of Nuclear Energy under Contracts No. DE-NE0008268 and DE-NE0000745 and by the National Academies Keck Futures Initiative.

This material is based upon work supported by the National Science Foundation Graduate Research Fellowship under Grant No. 1122374. Any opinion, findings, and conclusions or recommendations expressed in this material are those of the author(s) and do not necessarily reflect the views of the National Science Foundation.

The authors would like to thank Bo Paulson for his help in developing Figure 4, and Chukwunenye Anagbogu for his help in determining the relationships that govern the cost of XDPE chemical tanks.

7. Appendix

Table 3: Material costs for WUSABI construction, taken from [32] and adjusted to 2016 dollars

Material	**Cost**	**Unit**
Marine Grade Structural Steel	1.37	$/kg
HDPE Pipes	9.60	$/m
Adsorbent Support Rope	19.10	$/m
Platform Support Cable	21.10	$/m

Table 4: A comparison of chemical storage tank costs as a function of tank material

Tank	**Mass of Chemical Required per Tonne of Adsorbent or Exposure Time**	**Volume of Tank Required per Platform (m^3)**	**Steel Cost ($)**	**XDPE Cost ($)**
Elution Tank	24 hours	16.24	132,740	17,740
Bicarbonate Storage Tank	0.03	1.02	120,280	2,200
Regeneration Tank	3 hours	104.95	160,290	63,230
Alkaline Storage Tank	0.11	251	197,920	130,410
Product Storage Tank	0.09	3.74	121,120	3,590

Table 5: Cost break down of the top platform for the representative intermediary case.

Cost Component	**Overnight Capital Cost ($)**
Steel Structure	171,290
Platform Support Cable	24,170
Manufacturing Cost	195,470

Table 6: Cost break down of the bottom platform for the representative intermediary case.

Cost Component	**Overnight Capital Cost ($)**
Steel Structure	5,350
HDPE Rollers	4,240
Manufacturing Cost	9,600

Table 7: Total capital cost for the entire turbine field.

Cost Component	**Overnight Capital Cost ($)**
Top Platforms	39,093,080
Bottom Platforms	1,919,320
Adsorbent Net Support Rope	20,449,250
Fees to Wind Farm Owner	3,693,030
Ships	362,528,490

Table 8: Operating costs for the entire 1,200 tonne U/yr capacity field.[1]

Cost Component	**Annual Cost ($)**
NY Harbor #2 Heating Oil	11,526,560
Captain's Labor	955,040
Sailor/Workers Labor	12,364,320
Other Operating Consumables	23,904,600
Contingency	4,875,050

[1]Note that the optimum number of ships for this intermediary case is 8.

Table 9: Novel adsorbent production cost components specific to the WUSABI strategy.

Cost Component	**Unit Cost**	**Cost per Tonne Adsorbent ($)**
Net Structural Wire	$0.02/m	207.39
Net Fabrication Cost	$10.20/m	46.41

[1] Anirudhan, T. S., Tharun, A. R., Rijith, S., Suchithra, P. S., 2011. Synthesis and characterization of a novel graft copolymer containing carboxyl groups and its application to extract uranium (VI) from aqueous media. Journal of Applied Polymer Science 122 (2), 874–884.

[2] Byers, M., 2015. Optimization of the passive recovery of uranium from seawater. Master's thesis, The University of Texas at Austin.

[3] Byers, M. F., Haji, M. N., Slocum, A. H., Schneider, E., 2016. A Higher Fidelity Cost Analysis of Wind and Uranium from Seawater Acquisition symBiotic Infrastructure. Transactions of the American Nuclear Society 115, 271–274.

[4] Byers, M. F., Landsberger, S., Schneider, E., 2018. The use of silver nanoparticles for the recovery of uranium from seawater by means of biofouling mitigation. Sustainable Energy & Fuels.

[5] Byers, M. F., Schneider, E., 2015. Sensitivity of Seawater Uranium Cost to System and Design Parameters. In: GLOBAL 2015 21st International Conference & Exhibition: Nuclear Fuel Cycle for a Low-Carbon Future.

[6] Byers, M. F., Schneider, E., 2016. Optimization of the Passive Recovery of Uranium from Seawater. Industrial & Engineering Chemistry Research 55 (15), 4351–4361.

[7] Byers, M. F., Schneider, E., 2016. Uranium from Seawater Cost Analysis: Recent Updates. In: American Nuclear Society Annual Meeting Nuclear Power: Leading the Supply of Clean, Carbon Free Energy.

[8] Byers, M. F., Schneider, E., 2016. Uranium from Seawater Cost Analysis: Recent Updates. Vol. 116. pp. 85–88.

[9] Das, S., Oyola, Y., Mayes, R. T., Janke, C. J., Kuo, L.-J., Gill, G., Wood, J. R., Dai, S., 2016. Extracting Uranium from Seawater: Promising AF Series Adsorbents. Industrial & Engineering Chemistry Research 55 (15), 4110–4117.

[10] Davies, R. V., Kennedy, J., McIroy, R. W., Spence, R., Hill, K. M., 1964. Extraction of Uranium From Sea Water. Nature 203 (495), 1110–1115.

[11] Goodyear Tire & Rubber, 2003. Good Year Chemical Resistance Charts.

[12] Haji, M. N., 2017. Extraction of Uranium from Seawater: Design and Testing of a Symbiotic System. Ph.D. thesis, Massachusetts Institute of Technology.

[13] Haji, M. N., Byers, M., Schneider, E., Slocum, A. H., 2017. Cost Analysis of Wind and Uranium from Seawater Acquisition symBiotic Infrastructure using Shell Enclosures. Transactions of the American Nuclear Society 116, 89–92.

[14] Haji, M. N., Delmy, C., Gonzalez, J., Slocum, A. H., 2016. Uranium extraction from seawater using adsorbent shell enclosures via a symbiotic offshore wind turbine device. In: Proceedings of the 26th International Ocean and Polar Engineering Conference.

[15] Haji, M. N., Drysdale, J., Buesseler, K., Slocum, A. H., 2017. Ocean Testing of a Symbiotic Device to Harvest Uranium from Seawater through the Use of Shell Enclosures. In: Proceedings of the 27th International Ocean and Polar Engineering Conference.

[16] Haji, M. N., Gonzalez, J., Drysdale, J., Buesseler, K., Slocum, A. H., 2018. The effects of protective shell enclosures on uranium adsorbing polymers. under revision for Industry & Engineering Chemistry Research.

[17] Haji, M. N., Vitry, C., Slocum, A. H., 2015. Decoupling the functional requirements of an adsorbent for harvesting uranium from seawater through the use of shell enclosure. Transactions of the American Nuclear Society 113, 158–161.

[18] Hamlet, A. M., 2017. Uranium extraction from seawater: Investigating the hydrodynamic behavior and performance of porous shells. Master's thesis, Massachusetts Institute of Technology.

[19] Hu, J., Ma, H., Xing, Z., Liu, X., Xu, L., Li, R., Ling, C., Wang, M., Li, J., Wu, G., 2016. Preparation of Amidoximated UHMWPE Fiber by Radiation Grafting and Uranium Adsorption Test. Industrial & Engineering Chemistry Research 55, 4118–4124.

[20] Ineos Olefins and Polymers, 2012. Chemical Resistance Guide. Met. Finish. 96 (10).

[21] Kanno, M., 1984. Present status of study on extraction of uranium from sea water. Journal of Nuclear Science and Technology 21 (1), 1–9.

[22] Kim, J., Tsouris, C., Mayes, R. T., Oyola, Y., Saito, T., Janke, C. J., Dai, S., Schneider, E., Sachde, D., 2013. Recovery of Uranium from Seawater: A Review of Current Status and Future Research Needs. Separation Science and Technology 48, 367–387.

[23] Kuo, L.-J., Gill, G. A., Strivens, J., Schlafer, N., W. J., Wai, C. W., Pan, H.-B., ???? Assessment of Impacts of Dissolved Organic Carbon and Dissolved Iron Concentrations on Performance of Amidoxime-Based Adsorbent for Seawater Uranium Extraction, M3FT-17PN03020104.

[24] Kuo, L.-J., Gill, G. A., Tsouris, C., Rao, L., Pan, H.-B., Wai, C., Janke, C., Strivens, J., Wood, J., Schlafer, N., D'Alessandro, E., 2018. Temperature Dependence of Uranium and Vanadium Adsorption on Amidoxime-Based Adsorbents in Natural Seawater. Chemistry Select 3, 843.

[25] Kuo, L.-J., Pan, H.-B., Wai, C. M., Byers, M. F., Schneider, E., Strivens, J. E., Janke, C. J., Das, S., Mayes, R. T., Wood, J. R., Schlafer, N., Gill, G. A., 2017. Investigations into the Reusability of Amidoxime-Based Polymeric Adsorbents for Seawater Uranium Extraction. Industrial & Engineering Chemistry Research 56 (40), 11603–11611.

[26] Ladshaw, A. P., Wiechert, A. I., Das, S., Yiacoumi, A., Tsouris, C., 2017. Amidoxime Polymers for Uranium Adsorption: Influence of Comonomers and Temperature. Materials 10 (11), 1268.

[27] Levitus, S., Antonov, J. I., Baranova, O. K., Boyer, T. P., Coleman, C. L., Garcia, H. E., Grodsky, A. I., Johnson, D. R., Locarnini, R. A., Mishonov, A. V., Reagan, J. R., Sazama, C. L., Seidov, D., Smolyar, I., Yarosh, E. S., Zweng, M. M., 2013. The World Ocean Database. Data Science Journal 12, WDS229 – WDS234.

[28] Lindner, H., Schneider, E., 2015. Review of cost estimates for uranium recovery from seawater. Energy Economics 49, 9–22.

[29] Navigant Consulting, Inc., 2013. Offshore Wind Market and Economic Analysis. Tech. rep.

[30] Pan, H.-B., Wai, C. M., Kuo, L.-J., Gill, G., Tian, G., Rao, L., Das, S., Mayes, R. T., Janke, C. J., 2017. Bicarbonate Elution of Uranium

from Amidoxime-Based Polymer Adsorbents for Sequestering Uranium from Seawater. Chemistry Select 2 (13), 3769–3774.

[31] Park, J., Gill, G. A., Strivens, J. E., Kuo, L.-J., Jeters, R., Avila, A., Wood, J., Schlafer, N. J., Janke, C. J., Miller, E. A., Thomas, M., Addleman, R. S., Bonheyo, G., 2016. Effect Of Biofouling On The Performance Of Amidoxime-Based Polymeric Uranium Adsorbents. Industrial & Engineering Chemistry Research 55, 4328–4338.

[32] Picard, M., Baelden, C., Wu, Y., Chang, L., Slocum, A. H., 2014. Extraction of Uranium from Seawater: Design and Testing of a Symbiotic System. Nuclear Technology 188 (2), 200–217.

[33] Rothwell, G., 2016. Economics of Nuclear Power. Routledge.

[34] Schneider, E., Linder, H., 2014. Updates to the Estimated Cost of Uranium Recovery from Seawater. In: Proceedings of the 19th Pacific Basin Nuclear Conference.

[35] Schneider, E., Sachde, D., 2013. The Cost of Recovering Uranium from Seawater by a Braided Polymer Adsorbent System. Sci. Glob. Sec. 21 (2), 134–163.

[36] Seko, N., Katakai, A., Hasegawa, S., Tamada, M., Kasai, N., Takeda, H., Sugo, T., Saito, K., 2003. Aquaculture of uranium in seawater by a fabric-adsorbent submerged system. Nuclear Technology 144 (2), 274–278.

[37] Strivens, J. E., D'Alessandro, E., Schlafer, N., Kuo, L.-J., Wood, J., Flicker, M., Park, J., Gill, G. A., 2016. PNNL Marine Testing Program: Seawater Temperature Effect on Uranium and Trace Element Recovery in Sequim Bay (WA) and Southern Biscayne Bay (FL). Poster Presented at the International Conference on Seawater Uranium Recovery.

[38] Sugo, T., Tamada, M., Seguchi, T., Shimizu, T., Uotani, M., Kashima, R., 2001. Recovery System for Uranium from Seawater with Fibrous Adsorbent and Its Preliminary Cost Estimation. Journal of the Atomic Energy Society of Japan 43 (10), 1010–1016.

[39] Tamada, M., Seko, N., Kasai, N., , Shimizu, T., 2006. Cost estimation of uranium recovery from seawater with system of braid type adsorbent. Transactions of the Atomic Energy Society of Japan 5 (4), 358–363.

[40] Tularam, G. A., Ilahee, M., 2007. Environmental concerns of desalinating seawater using reverse osmosis. Journal of Environmental Monitoring 9 (8), 805–813.

[41] van Reis, R., Zydney, A., 2007. Bioprocess membrane technology. Journal of Membrane Science 297 (1), 16–50.

[42] World-Nuclear.org, 2016. Mixed oxide (mox) fuel. `http://www.world-nuclear.org/information-library/nuclear-fuel-cycle/fuel-recycling/mixed-oxide-fuel-mox.aspx`, Accessed: 2017-04-23.

[43] Xing, Z., Hu, J., Wang, M., Zhang, W., Li, S., Gao, Q., Wu, G., 2013. Properties and evaluation of amidoxime-based UHMWPE fibrous adsorbent for extraction of uranium from seawater. Science China Chemistry 56 (11), 1504–1509.

[44] Yamanaka, A., Izumi, Y., Kitagawa, T., Terada, T., Hirahata, H., Ema, K., Fujishiro, H., Nishijima, S., 2006. The effect of gamma-irradiation on thermal strain of high strength polyethylene fiber at low temperature. Journal of Applied Polymer Science 102, 204–209.

[45] Zhang, A., Asakura, T., Uchiyama, G., 2003. The adsorption mechanism of uranium (VI) from seawater on a macroporous fibrous polymeric adsorbent containing amidoxime chelating functional group. Reactive and Functional Polymers 57 (1), 67–76.

[46] Zhao, Y. N., Wang, M. H., Tang, Z. F., Wu, G. Z., 2010. Effect of gamma-ray irradiation on the structure and mechanical properties of UHMWPE fibers. Polymer Materials Science & Engineering 26, 32–35.